An indoor calibration light source of the transmissometers based on spatial light modulation[*]

LIANG Jing[1], ZHANG Guoyu[1,2,3]**, ZHANG Jian[1,2,3], XU Da[1,2,3], CHONG Wei[1,4], and SUN Jiliang[1]

1. *School of Opto-Electronic Engineering, Changchun University of Science and Technology, Changchun 130022, China*

2. *Opto-Electronic Measurement and Control Instrumentation, Jilin Province Engineering Research Center, Changchun 130022, China*

3. *Key Laboratory of Opto-Electronic Measurement and Optical Information Transmission Technology, Ministry of Education, Changchun 130022, China*

4. *Meteorological Observation Center, China Meteorological Administration, Beijing 100081, China*

Aiming at the problem that the calibration results of the transmissometers cannot be traced to the meteorological optical range (*MOR*) defined by the World Meteorological Organization (WMO). We designed an indoor calibration light source of the transmissometers based on spatial light modulation, focusing on the design of a non-intersecting Czerny-Turner spectroscopic system which achieved a spectral resolution of less than 1 nm in the range from 380 nm to 780 nm. Then, the calibration light source's spectrum matching model is established and the digital micromirror device (DMD)'s surface illuminance distribution law is simulated and analyzed. Finally, the *MOR* error of the calibrated light source is inverted. The results show that the simulation spectrum error of the 2 700 K absolute color temperature is below ±7.4% in the wavelength range from 380 nm to 780 nm, and the *MOR* error meets the requirements of the International Civil Aviation Organization in 40—2 000 m of *MOR*.

Document code: A **Article ID:** 1673-1905(2022)02-0065-7

DOI https://doi.org/10.1007/s11801-022-1112-z

Visibility represents the turbidity of the atmosphere or the transparency of the atmosphere. It is affected by climatic conditions such as haze, fog, rain, and snow, as well as air pollutants such as exhaust gas, smoke and dust, and has important value in forecasting weather processes and monitoring climate change. The World Meteorological Organization (WMO) introduced meteorological optical range (*MOR*) as the standard definition for measuring visibility. *MOR* refers to the length of the path through which the luminous flux of the parallel beam emitted by the incandescent lamp with 2 700 K color temperature is weakened by the atmosphere and reduced to 5% of the initial value[1].

At present, the main visibility measuring instruments are transmissometers and forward scatter meters. Because measurement process of the transmissometers is closely related to the *MOR*'s definition. Compared with other visibility measuring instruments, the transmissometers have higher measurement accuracy, especially when the visibility is low, so it is widely used in the measurement of parallel atmospheric visibility such as airport runways. The transmissometer is also used as a calibration instrument for the forward scatter meter[2,3].

However, the transmitting end light source of the transmissometers mostly uses halogen lamps, xenon pulse discharge tubes, white light emitting diodes (LEDs), monochromatic LED light sources, lasers, etc[4-6], which is different from the spectral distribution of 2 700 K color temperature's incandescent lamp, leading to the forward scatter meters cannot be traced to the *MOR* definition after calibration. Moreover, the external field calibration of the transmissometers is seriously affected by weather conditions. Therefore, the indoor calibration method of transmissometers has been widely studied. Among them, in 2006, the Royal Netherlands Meteorological Institute proposed a calibration method of the forward scatter meters using the transmissometers, forward scatter meters, neutral filter and standard scatterer[7]. This method can trace the *MOR* measurement value of the forward scatter meters to the spectral transmittance of the neutral filter indoors. In 2015, the Korea Research Institute of Standards and Science (KRISS)

---

proposed a 75 m baseline transmissometers' indoor calibration method traceable to the International System of Units[8], which traced the *MOR* measurement value to KRISS calibration result of spectral transmittance.

Although by using the neutral filter, the *MOR* measurement results of the transmissometers can be traced to the spectral transmittance, the neutral filters used by different manufacturers do not have a unified calibration device, and the calibration light source of the neutral filter is the spectral distribution of the International Commission on Illumination (CIE) standard illuminator A, which is different from the spectral distribution of 2 700 K color temperature's incandescent lamp, which still cannot be traced to the *MOR* definition.

Since the incandescent lamp is an isothermal radiation source[9], the spectral distribution of 2 700 K incandescent lamps can be equivalent to that of 2 700 K blackbody. At present, there are few studies on the spectral simulation of 2 700 K absolute color temperature in the range of 380—780 nm, but some progress has been made in the spectral simulation of the wide band. As the spectrum simulation technology of target color temperature becomes more and more abundant[10-13]. By 2020, in the spectral range of 500—800 nm, the spectral simulation accuracy of a specific color temperature has reached more than ±8%[14]. Judging from the current technical level, the spatial light modulation technology is the most suitable technical means for the simulation of the 2 700 K absolute color temperature's spectral distribution due to its high spectral simulation accuracy, low power consumption and small size.

Based on the current research status at home and abroad, there are no reports about 2 700 K absolute color temperature's spectrum simulation. Due to the lack of such light sources, the traceability chain of the transmissometers that meet the *MOR* definition cannot be established.

To this end, this paper designed a transmissometers' indoor calibration light source based on spatial light modulation. It will provide technical support for constructing a calibration system of the transmissometers that can be traced to the definition of *MOR*.

The indoor calibration light source of the transmissometers is mainly composed of fiber light source, Czerny-Turner spectroscopic system, digital micromirror device (DMD), focusing lens, integrating sphere, spectrometer and control and data processing system. The Czerny-Turner spectroscopic system is used for dispersion and light splitting, as shown in Fig.1.

The spectral range of the optical fiber light source selected is from 380 nm to 780 nm, the resolution of DMD is 1 920×1 080, and the pixel size is 7.56 μm. The broad-spectrum light beam emitted by the fiber light source is incident on the collimating mirror of the Czerny-Turner spectroscopic system through the slit. It is reflected by the collimating mirror to the grating, and after dispersion and light splitting, it is converged by the focusing mirror to the DMD surface array micro-mirror.

The DMD's switch is adjusted by the control and data processing system to modulate the spectral distribution. Then the focusing lens will converge the light beam into the integrating sphere for mixing, so as to realize the simulation of the 2 700 K absolute color temperature spectrum. The spectrum simulation result is collected by the spectrometer and sent to the control and data processing system.
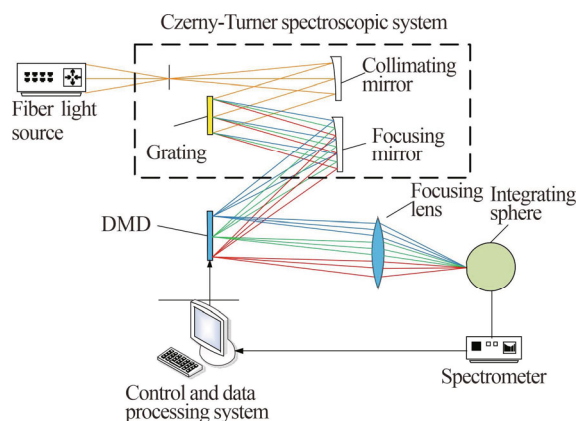

Fig.1 Schematic diagram of the indoor calibration light source of the transmissometers

The accuracy of spectral simulation mainly depends on the spectral resolution of the Czerny-Turner spectroscopic system. Czerny-Turner spectroscopic system mainly has three kinds of aberrations, namely spherical aberration, coma and astigmatism. Among them, the spherical aberration seriously affects the clarity of the contour of the spectral line and reduces the spectral resolution of the system. Coma causes unilateral diffusion of the profile of the spectral line, that is, one side of the spectral line is imaged clearly and the other side is blurred, which seriously affects the system's spectral resolution. Astigmatism will extend the spectral lines along the length of the slit, which will seriously affect the spatial resolution along the length of the slit. It is required that the spectral fitting units after dispersion by the Czerny-Turner spectroscopic system are arranged in sequence on the DMD array surface, that is, only the two-dimensional spectral resolution of the spectral line image is required, and there is no requirement for the spatial resolution of the spectral line image, so the correction of spherical aberration and coma only is considered.

According to the Rayleigh criterion, the formula for eliminating the spherical aberration of the Czerny-Turner spectroscopic structure is shown as

$$f \leq 256 \cdot \lambda \cdot F^4, \tag{1}$$

where $F=f/D$, f is the focal length of the collimating mirror, and D is the clear aperture.

According to Beulter light field function theory and Fermat principle[15,16], Czerny-Turner optical system coma can be divided into two parts. They are the width of the coma produced by the collimating mirror, denoted

as ε_1, and the width of the coma produced by the focusing mirror, denoted as ε_2, and the total coma of the system is $\varepsilon = \varepsilon_1 + \varepsilon_2$ at this time. Therefore, if $\varepsilon = 0$, the coma correction conditions of the Czerny-Turner optical structure are shown as

$$\frac{\sin(\alpha_2/2)}{\sin(\alpha_1/2)} = \frac{r_2^2}{r_1^2}\left(\frac{\cos i}{\cos\theta}\right)^3\left(\frac{\cos(\alpha_2/2)}{\cos(\alpha_1/2)}\right)^3, \tag{2}$$

where r_1 is the radius of the collimating mirror, r_2 is the radius of the focusing mirror, a_1 is the off-axis angle of the main ray on the collimating mirror, a_2 is the off-axis angle of the main ray on the focusing mirror, i is the incidence angle of the main ray on the grating, and θ is the diffraction angle of the center wavelength.

According to Eq.(2), only the non-intersecting Czerny-Turner structure can meet the astigmatism elimination condition, but Eq.(2) can only correct the coma at the center wavelength of the optical system. Due to the diffraction effect of the grating, the focusing mirror has different off-axis angles for different wavelengths of light. Therefore, the Czerny-Turner structure coma correction conditions of the wide-band spectrum can be transformed into the condition of eliminating coma at the center wavelength, looking for the position of a focusing mirror so that the off-axis angle of different wavelengths is approximately the same. The structural parameters of the optimized optical system are shown in Tab.1, the optical path is shown in Fig.2, and the plots of different fields of view and the variation of the root mean square (*RMS*) radius with wavelength are shown in Figs.3 and 4.

Tab.1 Structural parameters of the optical system

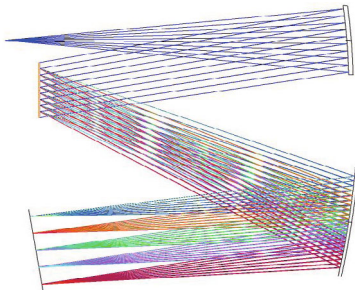| Parameter	Optimized structural value
r_1	86.6 mm
r_2	124 mm
a_1	2°
a_2	9°
i	10.03°
θ	31.08°

Fig.2 Light path diagram of the optimized Czerny-Turner structure

According to Figs.3 and 4, the Czerny-Turner spectroscopic system has good coma correction in the entire spectral range, and the spectral resolution of the central and edge wavelengths reaches 1 nm in the full field of view. The curve of the optical system *RMS* radius versus

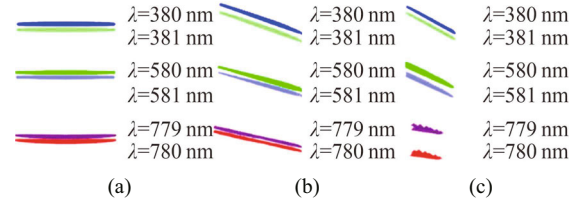wavelength shows that the spot size along the y direction is less than 6 μm in the entire spectrum range.

(a)   (b)   (c)

Fig.3 Point diagrams of different fields of view of the optical system: (a) 0 field of view; (b) 0.7 field of view; (c) 1.0 field of view
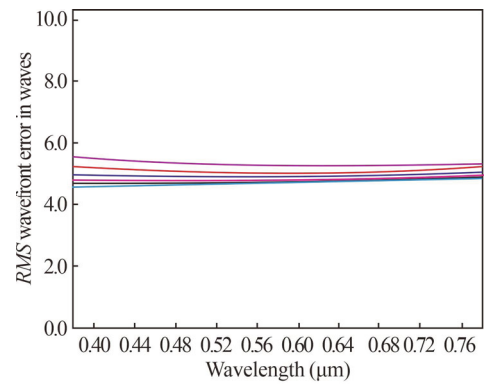

Fig.4 *RMS* radius variations with wavelength

Since the 2 700 K absolute color temperature's spectrum with a spectral range from 380 nm to 780 nm belongs to a continuous spectrum in the wide band, the method of superimposing a variety of spectral fitting units can be used to simulate the spectrum[17], and the principle of spectral superposition is shown as

$$S(\lambda_i) = \sum_1^i a_n s_n(\lambda_i), \tag{3}$$

where $S(\lambda_i)$ is the relative radiant energy at wavelength λ_i of the target spectrum, λ_i ranges from 380 nm to 780 nm, n is the number of spectral fitting units, a_n is the proportional coefficient of the spectral fitting unit, and $s_n(\lambda_i)$ is the relative radiant energy of the spectrum fitting unit's spectrum at wavelength λ_i.

The matrix form is expressed as

$$\begin{bmatrix} s_1(\lambda_1) & s_2(\lambda_1) & \cdots & s_{n-1}(\lambda_1) & s_n(\lambda_1) \\ s_1(\lambda_2) & s_2(\lambda_2) & \cdots & s_{n-1}(\lambda_2) & s_n(\lambda_2) \\ \vdots & \vdots & \vdots & \vdots & \vdots \\ s_1(\lambda_{i-1}) & s_2(\lambda_{i-1}) & \cdots & s_{n-1}(\lambda_{i-1}) & s_n(\lambda_{i-1}) \\ s_1(\lambda_i) & s_2(\lambda_i) & \cdots & s_{n-1}(\lambda_i) & s_n(\lambda_i) \end{bmatrix}\begin{bmatrix} a_1 \\ a_2 \\ \vdots \\ a_{i-1} \\ a_i \end{bmatrix} = \begin{bmatrix} s(\lambda_1) \\ s(\lambda_2) \\ \vdots \\ s(\lambda_{i-1}) \\ s(\lambda_i) \end{bmatrix}. \tag{4}$$

After the spectral fitting unit is determined, the fitting spectrum can be obtained by solving the generalized least squares solution of the scale coefficient of the spectral fitting unit that meets the over-determined equation group according to Eq.(4).

In order to be traced to the definition of *MOR*, the spectral distribution of the transmissometers' calibration light source needs to match the absolute color temperature of

2 700 K. Therefore, it is necessary to establish a calibration light source's spectral matching model.

The transmissometers directly measure the atmospheric transmittance τ caused by the scattering and absorption between the optical transmitter and the optical receiver at the baseline distance L, and the MOR[2] is calculated as

$$MOR = \frac{L \ln 0.05}{\ln \tau}. \tag{5}$$

Due to the optical properties of the atmosphere, the spectral transmittance in the visible light region is different[18]. At this time, the relationship between the atmospheric spectral transmittance $\tau(\lambda)$ and the atmospheric transmittance τ is

$$\tau = \frac{\int_{380}^{780} \tau(\lambda)S(\lambda)V(\lambda)\mathrm{d}\lambda}{\int_{380}^{780} S(\lambda)V(\lambda)\mathrm{d}\lambda}, \tag{6}$$

where $S(\lambda)$ is the spectral distribution of the calibration light source, λ is the wavelength of visible light from 380 nm to 780 nm, and $V(\lambda)$ is the visual function of the human eye. The atmospheric transmittance error caused by the difference between the spectral distribution of the calibration light source and the 2 700 K absolute color temperature's spectral distribution makes the MOR unable to be traced to the WMO definition accurately. Therefore, the spectral simulation error will affect the calibration of the transmissometers.

Differentiating Eq.(5), and ignoring the error of the baseline length, when the luminous intensity of the light source at the receiving end is stable, the relationship between the atmospheric transmittance error and the visibility error can be obtained as

$$\mathrm{d}\tau = -\frac{L \ln 0.05}{MOR} \cdot \mathrm{e}^{\frac{L \ln 0.05}{MOR}} \cdot \frac{\mathrm{d}MOR}{MOR}. \tag{7}$$

The transmissometers are widely used to measure the runway visual range (RVR) of airports. International Civil Aviation Organization (ICAO) stipulates that the RVR measurement range needs to cover a visibility range from 50 m to 1 500 m[19]. Therefore, we define the MOR range from 40 m to 2 000 m. The ICAO's recommended MOR accuracy standard is used as the MOR error standard to establish the basis for the spectrum matching of the calibration light source. The ICAO's recommended MOR accuracy standard[19] is: if MOR is up to 600 m, the absolute error dMOR is ±50 m; the relative error dMOR/MOR is within ±10% between 600 m and 1 500 m; the relative error dMOR/MOR is within ±20% above 1 500 m.

The typical baseline length and MOR range of the transmissometers are substituted into Eq.(7) to meet the accuracy requirements of the three categories of MOR recommended by ICAO respectively, and then the maximum allowable error of atmospheric transmittance can be obtained as shown in Tab.2.

According to the MOR definition, the atmospheric transmittance τ_0 corresponding to the 2 700 K incandes-

cent light source is 5%, and spectrum matching basis of the transmissometers' calibration light source is

$$\frac{\int_{380}^{780} \tau_0(\lambda)S(\lambda)V(\lambda)\mathrm{d}\lambda}{\int_{380}^{780} S(\lambda)V(\lambda)\mathrm{d}\lambda} - \tau_0 \leq \mathrm{d}\tau_{max}, \tag{8}$$

where $\tau_0(\lambda)$ is the atmospheric spectral transmittance when MOR is defined.

Tab.2 The atmospheric transmittance's maximum allowable errors corresponding to different baseline lengths

Baseline length (m)	Maximum allowable error
10	±0.001 9
20	±0.003 8
30	±0.005 6
50	±0.008 9

The composition of the atmosphere contains different molecules. Although their light absorption capacity is different, the composition is relatively stable. Therefore, under the six typical atmospheric environmental conditions, the change trend of the transmittance in the visible light band is basically the same[20].

In order to obtain the atmospheric spectral transmittance curve with an integrated transmittance of 5% when the visibility is defined, the average spectral transmittance values are adjusted under six atmospheric conditions, as shown in Fig.5.
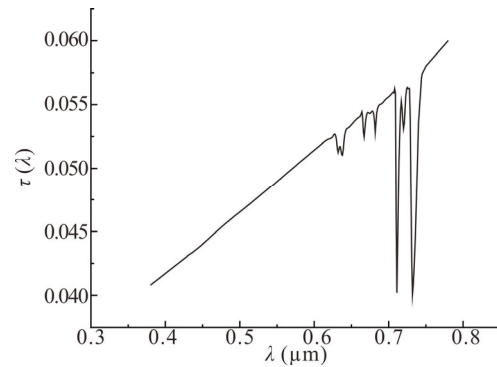

Fig.5 Simulated spectral transmittance

According to Eq.(5), the atmospheric spectral transmittance changes within the visible light wavelength range, and in the short-wavelength region of visible light, the change is gentle, and the transmittance slowly increases with the increase of wavelength. When it is close to the red light band (630—780 nm), the several absorption peaks have appeared. The spectral transmittance is the smallest near 710 nm and 730 nm. This is because the absorption of atmospheric molecules has very obvious selectivity[21]. In the visible light band, the main absorption gases are oxygen and water vapor. The troughs

near 630 nm, 660 nm and 680 nm are mainly caused by oxygen, and the troughs near 710 nm and 730 nm are basically caused by water vapor.

According to Eq.(4), the distribution law of relative illuminance on the DMD surface determines the selection of the weight coefficient of the spectral fitting unit in the spectral superposition process. Therefore, accurate acquisition of the illuminance distribution law is of great significance for improving the accuracy of spectral simulation and computing efficiency. In the Lighttools software, the spectral characteristics of the xenon lamp fiber light source in the range of 380 nm to 780 nm are used to model with the optimization and design of the Czerny-Turner spectroscopic system, and then the distribution law of the DMD surface illuminance is simulated and analyzed. The simulated light path is shown in Fig.6.
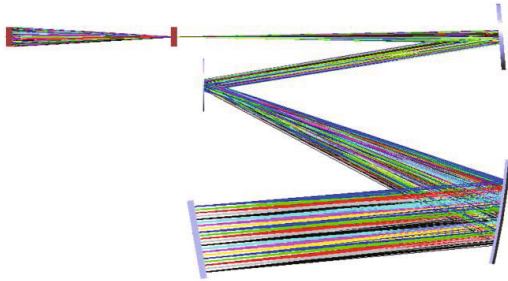

**Fig.6 Simulated light path of the DMD surface illuminance distribution law**

The simulation results of the relative luminance distribution and the dispersive illuminance distribution on the surface of the DMD are shown in Fig.7.

Fig.7 shows that when the dispersion wavelength is the same (the *Y*-axis coordinate is the same), the illuminance in the middle area of the DMD surface is the highest, and it gradually decreases to the two sides; when the column coordinates of the DMD micro-mirrors are the same (the *X*-axis coordinates are the same), the DMD surface illuminance distribution shows a downward trend from 380 nm to 780 nm. Therefore, according to Eq.(4), when solving the least squares solution of the 2 700 K absolute color temperature's spectral simulation, adjust the weight coefficient of the spectral fitting unit according to this law, and a better spectral simulation result can be obtained.

We use the principle of spectral superposition based on the least square method to modulate the spectrum. Without considering the diffraction characteristics, according to the principle of spectral superposition formula and the law of DMD surface illuminance distribution, the correctness of the spectral simulation can be verified.

A convergent lens and an integrating sphere are added to the simulation model of the DMD surface illuminance distribution law, and the diameter of the focusing lens is 18 mm, the focal length is 24 mm, the diameter of the inner wall of the integrating sphere is 26 mm, and then

the overall model of transmissometers' indoor calibration light source is obtained, as shown in Fig.8.
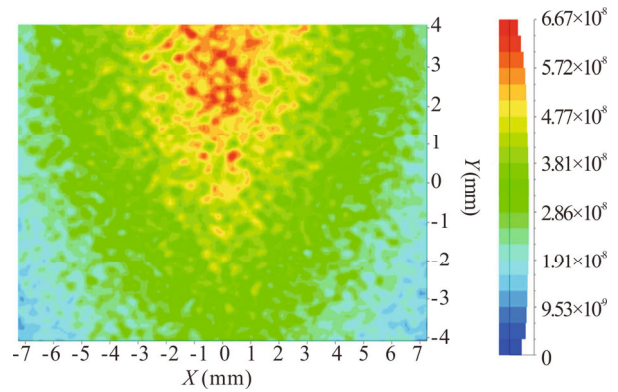
(a) Relative illuminance distribution
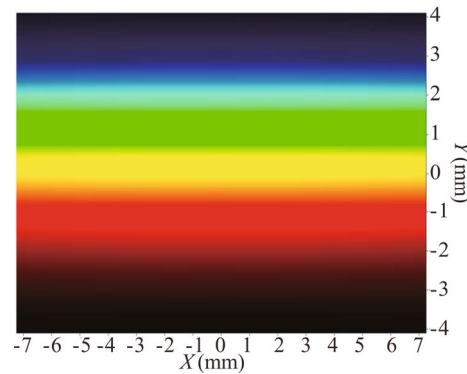
(b) Dispersive illuminance distribution

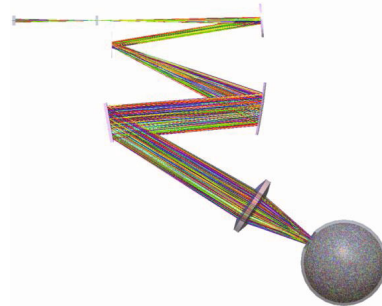**Fig.7 Distribution law of DMD surface illuminance**

Fig.8 Overall simulation model of the indoor calibration light source of the visibility observation instrument

The fitted spectral distribution is modulated, and the energy ratio of the spectral basic simulation unit is adjusted by controlling the state of the DMD switch, so that the adjusted spectral distribution meets the spectral matching basis of the calibration light source in Eq.(8), thus, the spectrum simulation of the 2 700 K absolute color temperature is completed.

The spectral simulation error p is used to evaluate the quality of spectral matching. It is the maximum value of the ratio of the difference between the simulation spectral distribution $S(\lambda_i)$ and the target spectral distribution $S_0(\lambda_i)$

to the target spectral distribution in the range of 380—780 nm.

$$p = \text{MAX}\left[\frac{S(\lambda_i) - S_0(\lambda_i)}{S_0(\lambda_i)}\right] \times 100\%. \tag{9}$$

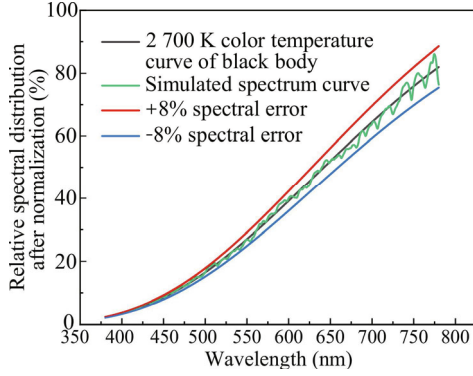The spectrum simulation result is shown in Fig.9, and the relative error is shown in Fig.10.

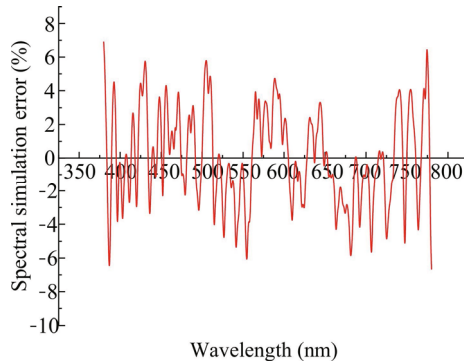**Fig.9 Spectrum simulation results of 2 700 K color temperature**

Fig.10 Spectral simulation relative error of 2 700 K color temperature

According to Fig.9 and Fig.10, the relative error of the spectral simulation in the range from 380 nm to 780 nm is within ±7.4%.

Substituting the simulation spectral distribution $S(\lambda_i)$ into Eq.(6), the atmospheric transmittance is 5.17%, and the atmospheric transmittance error is 0.001 7. According to Eq.(7), the *MOR* error of the calibration light source's spectrum in the range of 40—2 000 m *MOR* is inverted. Finally, we compared the *MOR* error with the ICAO's recommended standard. In the range of 600—2 000 m *MOR*, the *MOR* measurement accuracy recommended by ICAO is expressed as absolute error. The comparison result is shown in Fig.11.

According to Fig.11, the *MOR* errors of the simulated spectrum are all within the *MOR* measurement accuracy requirements recommended by ICAO. The *MOR* error at the 50 m baseline showed a U-shaped distribution, and the error was the smallest at the 73 m *MOR*. After the 125 m *MOR*, the *MOR* error decreases with the increase

of the baseline length, so the *MOR* error can be reduced by expanding the baseline length.

(a) In *MOR* of 40—2 000 m
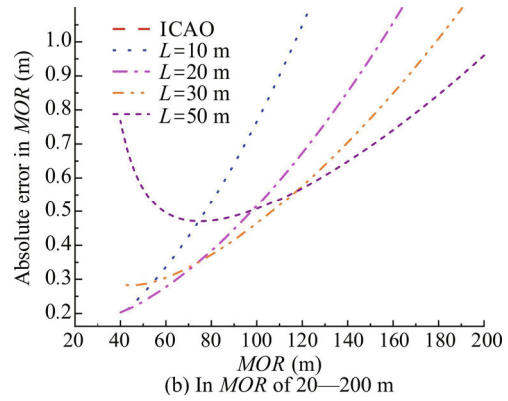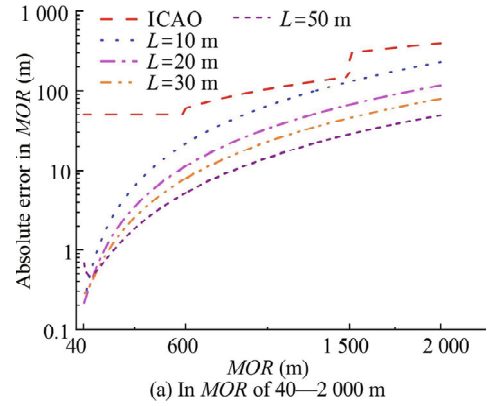

(b) In *MOR* of 20—200 m

Fig.11 *MOR* inversion results

This paper designed an indoor calibration light source of the transmissometers based on spatial light modulation. A Czerny-Turner spectroscopic system with a spectral resolution of less than 1 nm in the range from 380 nm to 780 nm was optimized and designed. The optimal combination of fitting spectral coefficients was solved by using the principle of spectral superpostion, and the spectral matching model of the calibration light source was established to achieve the spectral simulation error of 2 700 K absolute color temperature in the range from 380 nm to 780 nm is ±7.4%. The *MOR* error of the calibration light source spectrum in the range of 40—2 000 m *MOR* is retrieved, which meets the requirements of ICAO. It provides theoretical basis and research methods for constructing the traceability chain of *MOR* calibration and the calibration system of the transmissometers.

Statements and Declarations

The authors declare that there are no conflicts of interest related to this article.

References

[1]   World Meteorological Organization. Guide to meteorological instruments and methods of observation[R].

Geneva：WMO, 2014：291.

[2]   CHONG W, BIAN Z Q, CHU J H, et al. A method for calibrating forward scatter meters indoors[J]. Metrologia, 2020, 57(6)：065030.

[3]   CHU J H, TANG X X, WANG H. Research on the calibration technology of visibility based on artificial simulated environment[C]//2019 International Conference on Meteorology Observations, December 28-31, 2019, Chengdu, China. New York：IEEE, 2019.

[4]   LI X B, GONG C W, XU Q S, et al. The correlation between fine aerosol particles and visibility[J]. Optics and precision engineering, 2008, 16(07)：1177-1180.

[5]   XU H T. Basic functions and applications of LT31 atmospheric transmissometer[J]. China new telecommunications, 2014, 16(03)：67-67.

[6]   TANG H Q, JU L, BAO T T. Design of WSN-based transmissive visibility detection system[J]. Instrument technology and sensors, 2011(11)：57-59.

[7]   BLOEMINK H I. KNMI visibility standard for calibration of scatterometers[C]//4th International Conference on Experiences with Automatic Weather Stations, 2006, Lisboa, Portugal.

[8]   PARK S, LEE D H, KIM Y G. SI-traceable calibration of a transmissometer for meteorological optical range (MOR) observation[J]. Hankook kwanghak hoeji, 2015, 26(2)：73-82.

[9]   WU Z F, DAI C H, YU J L, et al. Performance investigation of blackbody BB3500M and temperature measurement[J]. Journal of applied optics, 2012, 33(5)：926-930.

[10]   FRYC I, BROWN S W, OHNO Y. Spectral matching with an LED-based spectrally tunable light source[J]. Proceedings of SPIE the international society for optical engineering, 2005, 5941：300-308.

[11]   ZHANG X J, ZHANG G Y, SUN G F, et al. Study on the spectrum of a star simulator based on mixed light sources[J]. Acta photonica sinica, 2014, 43(2)：33-38. (in Chinese)

[12]   LIU H X, REN J W, LIU Z X, et al. Multi-color temperature and multi-magnitude single-star simulator based on LED[J]. Chinese journal of optics, 2015, 35(2)：179-186.

[13]   ARTURAS B, ALGIRDAS N, ALGIRDAS M, et al. Compact hybrid solar simulator with the spectral match beyond class A[J]. Journal of photonics for energy, 2016, 6(3)：035501.

[14]   XU D, YUE S X, ZHANG G Y, et al. Design of offner convex grating wide dynamic range radiation calibration light source[J]. Chinese optics, 2020, 13(5)：1085-1093.

[15]   NAMIOKA T. Theory of the concave grating. III. Seya-Namioka monochromator[J]. Journal of the optical society of America (1917-1983), 1959, 49(10)：951-959.

[16]   WALL C F, HANSON A R, TAYLOR J, et al. Construction of a programmable light source for use as a display calibration artifact[J]. International society for optics and photonics, 2001, 4295：259-266.

[17]   ZHANG J, SUN J L, ZHANG G Y, et al. Study on 2700 K blackbody color temperature spectral simulation method for visibility calibration[J]. Meteorological, hydrological and marine instruments, 2020, 37(04)：8-10.

[18]   ARNULF A, BRICARD J, CURD E, et al. Transmission by haze and fog in the spectral region 035 to 10 microns[J]. Journal of the optical society of America, 1957, 47(6)：491-498.

[19]   International Civil Aviation Organization. Annex 3 to the convention on international civil aviation：meteorological service for international air navigation[R]. Montreal：ICAO, 2007：ATT A-1.

[20]   WANG X W, ZHOU Z H, BAI J, et al. Research on the influence of atmospheric environment on the transmission characteristics of visible light[C]//The 31st Annual Meeting of the Chinese Meteorological Society, November 3-5, 2014, Beijing, China. Beijing：CMS, 2014：158-166.

[21]   LIANG W H, WANG Y J, YANG X L, et al. Design of light waves atmospheric transmittance model based on MODTRAN[J]. Laser & infrared, 2016(12)：1531-1535. (in Chinese)